Report on FY17 Testing in Support of Integrated EPP-SMT Design Methods Development

Yanli Wang
Robert I. Jetter
T.-L. Sham

August 1, 2017

OAK RIDGE NATIONAL LABORATORY
MANAGED BY UT-BATTELLE FOR THE US DEPARTMENT OF ENERGY

Materials Science and Technology Division

REPORT ON FY17 TESTING IN SUPPORT OF INTEGRATED EPP-SMT DESIGN METHODS DEVELOPMENT

Yanli Wang, Robert I. Jetter* and T.-L. Sham†

* RI Jetter Consulting
†Argonne National Laboratory

Date Published: August 1, 2017

CONTENTS

LIST OF FIGURES

LIST OF TABLES

ACRONYMS

ART	Advanced Reactor Technologies Program
ASME	American Society of Mechanical Engineers
B&PV	Boiler and Pressure Vessel
CC	Code Case
CF	Creep-Fatigue
DOE	Department of Energy
EPP	Elastic-Perfectly Plastic
ORNL	Oak Ridge National Laboratory
SMT	Simplified Model Test

ACKNOWLEDGMENTS

ABSTRACT

The goal of the proposed integrated Elastic Perfectly-Plastic (EPP) and Simplified Model Test (SMT) methodology is to incorporate a SMT data-based approach for creep-fatigue damage evaluation into the EPP methodology to avoid the separate evaluation of creep and fatigue damage and eliminate the requirement for stress classification in current methods; thus greatly simplifying evaluation of elevated temperature cyclic service. The purpose of this methodology is to minimize over-conservatism while properly accounting for localized defects and stress risers. To support the implementation of the proposed methodology and to verify the applicability of the code rules, thermomechanical tests continued in FY17. This report presents the recent test results for Type 1 SMT specimens on Alloy 617 with long hold times, pressurization SMT on Alloy 617, and two-bar thermal ratcheting test results on SS316H at the temperature range of 405 ^{0}C to 705 ^{0}C. Preliminary EPP strain range analysis on the two-bar tests are critically evaluated and compared with the experimental results.

1. BACKGROUND

The goal of the EPP-SMT approach is to incorporate an SMT data-based approach for creep-fatigue (CF) damage evaluation into the EPP methodology to avoid the use of the "D" diagram and to minimize over-conservatism while properly accounting for localized defects and stress risers. There are two approaches of interest to the proposed integrated evaluation of cyclic service life that have received attention over the last several years. One of these approaches is identified as the Elastic-Perfectly Plastic (EPP) methodology and the other is identified as the Simplified Model Test (SMT) methodology. The EPP cyclic service methodology greatly simplifies the design evaluation procedure by eliminating the need for stress classification that is the basis of the current rules. However, the EPP methodology for evaluation of creep-fatigue damage still requires the separate evaluation of creep damage and fatigue damage by placing a limit on the allowable combined damage, the "D" diagram based on calculating individual creep and fatigue damages.

A detailed plan in developing this methodology has identified the key issues, assumptions and the proposed path to resolution and verification of the EPP-SMT approach. EPP-based design methods have already been qualified for ASME Sec. III Div. 5 applications via approved two code cases: strain limits code case (EPP strain limits CC N-861) and EPP creep-fatigue code case (EPP C-F CC N-862). Fig. 1 is an updated flow chart from the initial plan (Wang, et. al., 2016, Wang, et. al., 2017b) and it shows the impact of recent test results from pressurization SMT and the EPP strain range analysis. The major elements in this flow chart include: three key assumptions that have been made to move forward; the near-term test and evaluation actions required to validate these assumptions; and the lon-term test and analytical development required depending upon the outcome of the near term validation efforts.
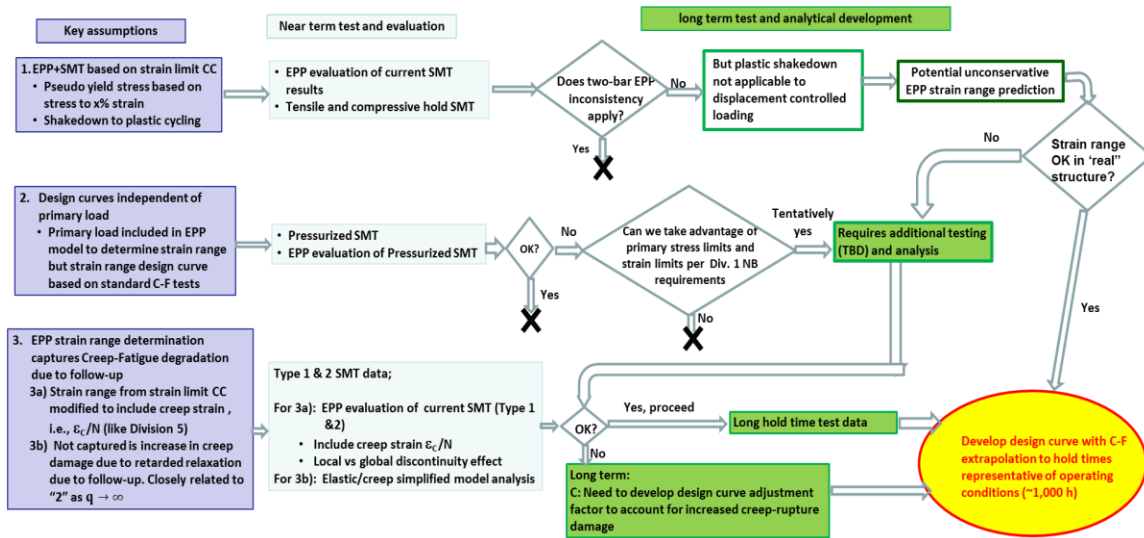
Fig. 1. Updated flow-chart on the development of the EPP-SMT approach.

Shown under the category of "Near-term test and evaluation" for assumption 1, is a comparison of tension hold data with data from tests with alternating tension and compression hold times. The reason for this is twofold. First, it would be desirable to base the validation on the more conservative data. However, perhaps the more important reason is to minimize the barreling effect that clouds the interpretation of the tension-hold only test data.

Pressurized SMT capsule tests are being used to assess the second assumption that the stress level associated with primary loading will be small compared with the secondary and peak stress levels and

shouldn't have a significant effect on the total life. In addition to the pressurized SMT data, the modified two-bar test with one bar as SMT specimen at constant temperature and the second bar a smooth gage geometry, under Long-Term Tests, will provide valuable data for verification of the effects of superimposed primary loading. The advantage of this two-bar modified configuration is that all the relevant test parameters can be measured directly. If it turns out that the effect of primary loading is significant, then the proposed solution, as shown under the long-term test and analytic development column, is to develop mean stress type design curves analogous to the mean stress correction curves for the fatigue evaluation of some materials below the creep regime.

The third assumption, that the EPP strain range determination captures the creep-fatigue degradation due to follow-up effects, will be evaluated using results from both the Type 1 and 2 SMT test specimens to determine if adjustment factors will be required for the SMT based design curves

Longer term tests are required to develop the SMT design curves and to support the development of adjustment factors to account for such effects as sustained primary loading and retardation of stress relaxation due to follow-up, if needed.

This report presents the recent SMT test results on Alloy 617 and two-bar thermal ratcheting test results on SS316H. Preliminary EPP strain range analysis on the two-bar tests are critically evaluated. The tests and analysis in this report are critical in developing of this integrated EPP-SMT design approach.

2. EXPERIMETNAL DETAILS

2.1 SMT AND PRESSURIZED SMT FOR ALLOY 617

All the SMT and pressurized SMT experiments performed in this study used the same Alloy 617 plate from Heat 314626 from ThyssenKrupp VDM USA, Inc., with nominal thickness of 1.5". The plate allows one of the SMT solid bar specimen and tubular pressurization specimen be prepared from the thickness. The chemical composition of the plate is listed in Table 1. The specimen longitudinal direction is oriented with the rolling direction of the plate. All the specimens were tested in the as-received condition.

Table 1. Chemical compositions of Alloy 617 plate with heat number 314626 (weight %).

C	S	Cr	Ni	Mn	Si	Mo	Ti	Cu	Fe	Al	Co	B
0.05	<0.002	22.2	R54.1	0.1	0.1	8.6	0.4	0.04	1.6	1.1	11.6	<0.001

The gage test section of the Type 1 SMT geometry specimens shown in Fig. 2 was the same as what was previously tested for Type 1 SMT on Alloy 617. The tab diameter was reduced to better utilize supply material plate. The control length for the applied displacement was 5 in to achieve the designed elastic follow up. The average strain was measured using a 0.4 in gage extensometer placed inside the necked test section. The measured axial strains were used to generate the hysteresis loops along with the applied stresses.
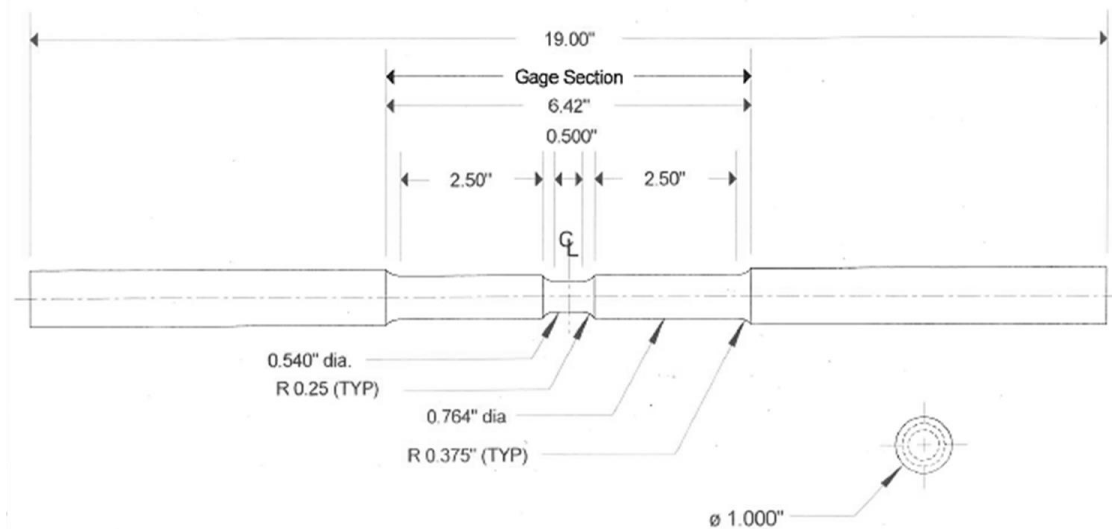
Fig. 2. Type 1 SMT solid bar specimen geometry for Alloy 617. Units are in inches.
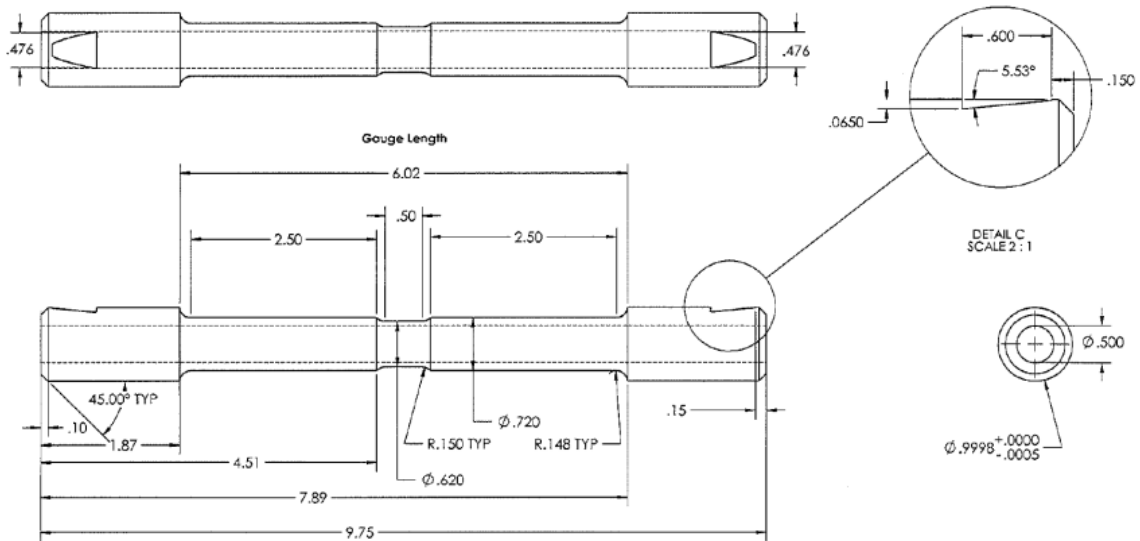
Fig. 3. Center test section of the pressurization SMT specimen for Alloy 617. Units are in inches.

There are two types of end-displacement profiles used for the SMT creep-fatigue testing in this report, and they are fully reversed loading with peak tension hold or combined peak tension and peak compression hold (schematically shown in Fig. 4). The loading was automated through a LabVIEW program. The loading segment was 3 s, and the same unloading rate was applied. For the experiments with hold times for 600 s (10 min), 1,800 s (30 min) and 36,000 s (10 hr) on Type 1 SMT, tension only profile shown in Fig. 4a was used. The pressurized SMT test on INC617-P09 used a tension hold of 600 s (10 min) loading (Fig. 4a), and combined tension hold and compression hold of 600 s (10 min) each (Fig. 4b). The combined tension and compression hold was to minimize the barreling of the necked test section shown in the previous tension hold tests (Wang, et. al., 2016).

(a)

(b)
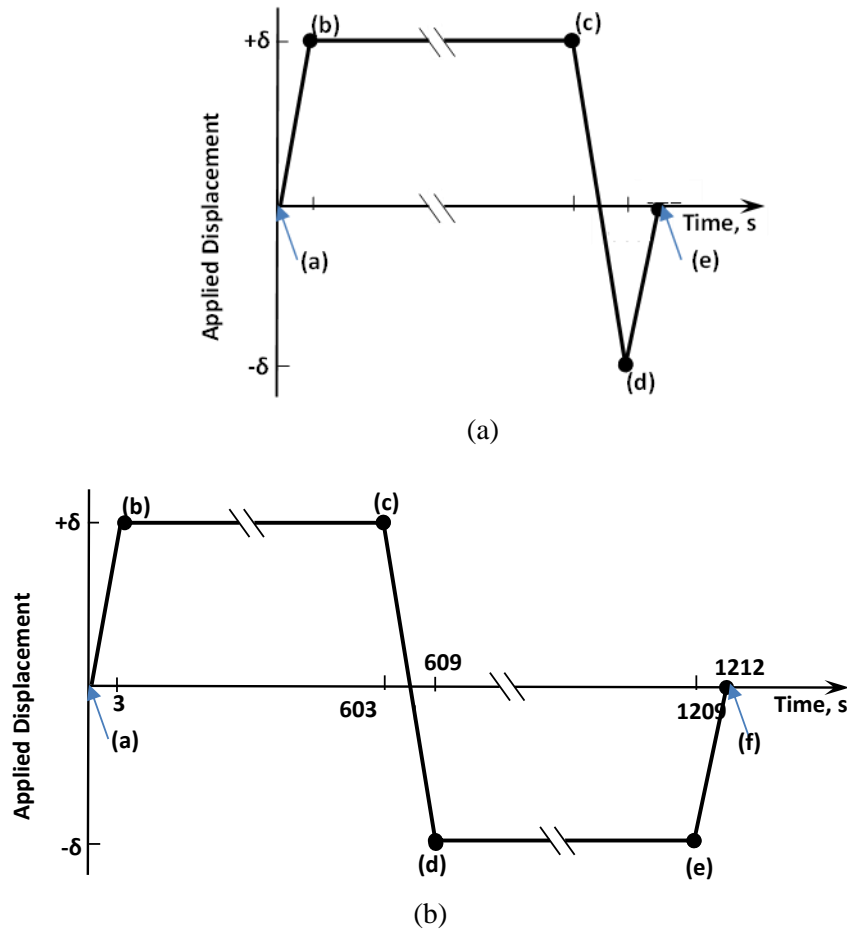
Fig. 4. Applied end-displacement profile for one cycle of SMT creep-fatigue testing with tension hold (a) and combined tensile-compression hold (b).

2.2 TWO-BAR THERMAL RATCHETING ON SS316H

2.2.1 Two-bar thermal ratcheting experiment

316H stainless steel (SS316H) was chosen for the experiment primarily because it has been well characterized and it is a material of interest for advanced reactor systems. SS316H round bar material with nominal diameter of 1 in was previously purchased from Outokumpu Stainless Bar, LLC. The heat number is 101076 and the as-received SS316H bar satisfies specification ASME SA497. The chemical composition of the SS316H is listed in Table 2. All the specimens were tested in the as-received condition. The specimen geometry is shown in Fig. 5.

Table 2. Chemical compositions of SS316H bar with heat number 101076 (weight %).

C	P	Si	Ni	Mn	N	Ti	Sn	V	Fe	Cb-Ta
0.045	0.028	0.650	10.120	1.420	0.053	0.002	0.006	0.060	balance	0.014
S	**Cr**	**Co**	**Mo**	**Nb**	**Al**	**B**				
0.024	16.230	0.279	2.090	0.014	0.004	0.004				
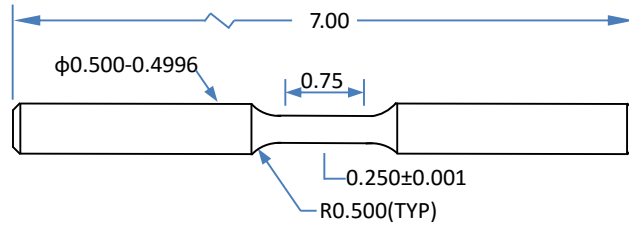
Fig. 5. Specimen geometry the SS316H used in two-bar thermal ratcheting experiments. Units are in inches.

The experimental control logic used is similar to what was previously reported by Swindeman et al. (1982) and is explained in detail in Wang et al. (2013a, 2015, 2016). In this method, two coupled servo-controlled machines are used to implement two bars in a parallel testing condition and the control system forces equal strains in the two specimens, yet allows the applied total load to be constant. The two bars are installed in two, coupled, servo-hydraulic machines with machine #1 under strain control and machine #2 under load control. The strain signals measured by the extensometer on Bar 2 are fed into machine #1 as the command signal for strain control of Bar 1. This control logic ensures equal amount of deformation for the two bars at all time. The driving force for the specimens to experience deformation is the constant total load of the two bars and the cyclic temperature profile applied to each bar. A two-bar model is a simplified analysis of a vessel under a combination of a constant, primary pressure load and a secondary, alternating thermal cycle. The two bars represent two extreme material fibers (see Fig. 6).
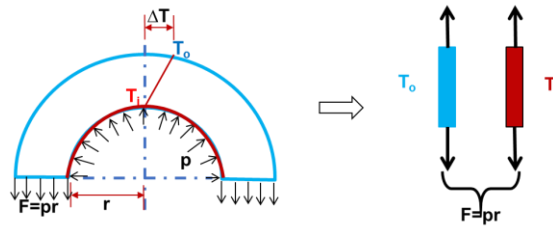
Fig. 6. Pressurized cylinder with radial thermal gradient represented by a two-bar model.

Fig. 7 shows the two-bar thermal cycle. The thermal strains in the specimen are a function of the time delay between ③ to ⑤, the cooling rate and the total temperature difference. The heating and cooling rates were 30 °C/min. Table 3 has summarized the parameters used for the two-bar experiments and EPP analysis. Experiments were performed on one set of specimens at the temperature range of 405 °C to 705 °C with different combinations of total load levels and time delays. The changing of loading conditions was performed at 405 °C without unloading the specimens to zero load from the previous condition.
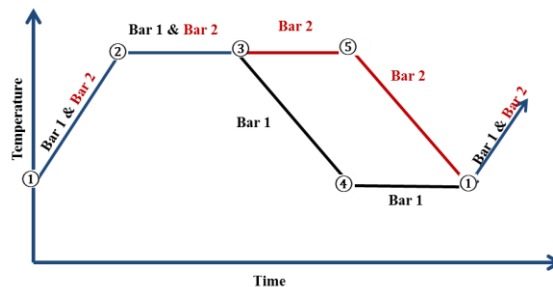
Fig. 7. Two-bar thermal cycle.

Table 3. Parameters of the two-bar experiment and EPP analysis.

Material	SS316H
Specimen diameter	0.25 in
Temperature range	405 ºC to 705 ºC
hold time ② to ③	60 min
Heating and cooling rate ① to ②; ③ to ④ and ⑤ to ①	30 ºC/min
time delay, ③ to ⑤	From 1 min to 10 min
Applied total load	From -1,000 lbs to 1,000 lbs

Consistent with the preceding work by Wang et al. (2013a, 2014, 2015, 2016), the ratcheting strain is defined as the difference in the mechanical strain at a time point in a thermal cycle and that at the same time point in the reference cycle. When the same reference point in the thermal cycle is selected, the amount of ratcheting strain calculated based total strain is the same as that calculated based on mechanical strain. In this study, the ratcheting strains were calculated from the maximum total strains of each cycle, and they were approximately the same values when calculated based on the minimum strains. It was also observed that the cyclic ratcheting rates were approximately constant and the shape of the hysteresis loops were uniform for all the tests conducted after the first six initial cycles. In this study, the ratcheting rates were evaluated using the sixth cycle as the reference cycle, and the results were extrapolated to obtain the ratcheting strain at 200 hr to provide information to our parallel theoretical studies on strain limits of SS316H.

2.2.2 EPP strain limits analysis

The EPP method assumes that the average deformations computed for a system with an elastic-perfectly plastic analysis using a material's elastic properties and a pseudo-yield stress less than the minimum flow stress the material experiences over its design life will be greater than the actual, experimental deformations. The EPP strain limits code case (ASME B&PV Code Case N-861) sets this temperature dependent pseudo-yield stress based on the isochronous stress/strain curves for the material defined in the ASME code.

The code case uses this bounding EPP analysis to evaluate designs against the limits on inelastic strain established in the ASME code. Essentially the code case sets two conditions on the results of the analysis:

- the structure must shake down under cyclic loading with no cyclic deformation using a target pseudo yield stress less than or equal to the membrane strain limits of 1% for base material and 0.5% for weldments

- if the structure shakes down, the inelastic strain computed by adding inelastic strain from the elastic-perfectly plastic analysis to the afore mentioned target strain must be less than the strain limits.

If a structure meets both these criteria then, by the bounding principal outlined above, the true structure will both shake down and accumulate less than 1% inelastic strain over its design life. Therefore, the code case deems it to have met the strain limits requirements of Section III, Division 5, HBB-T-1310.

This work also uses the EPP strain limits analysis procedure in a slightly different way. Here we compare the strain range computed from EPP analysis to the experimental strain ranges found in corresponding experiments. The idea is that the strain range computed by the elastic-perfectly plastic analysis with an

appropriate temperature-dependent pseudo-yield stress established from the code isochronous curves should be greater than the true experimentally measured strain ranges.

3.   RESULTS AND DISCUSSIONS

3.1   SMT TEST RESULTS ON ALLOY 617

### 3.1.1   Hold time effect on type 1 SMT - Alloy 617

The conventional creep-fatigue interaction diagram is generated using strain-controlled fatigue tests with variable strain ranges and hold times in tension and compression. Lower strain ranges and longer hold times increase creep damage, whereas, fatigue dominates at higher strain ranges and short hold times. Changes in dominating damage mode in creep-fatigue experiments are often accompanied with differences in failure mode which can be confirmed by evidence of creep cavitation and/or fatigue cracking. As the hold time is increased, the strain-controlled creep-fatigue cycle life will approach saturation and the stress relaxation process saturates and the stress reaches a constant value. For creep-fatigue experiments with very long hold time and only occasionally imposed cycles, the process can be treated as pure stress relaxation. For standard strain controlled creep-fatigue on Alloy 617 at 950 ^{0}C, Carrol et. al. (2011) demonstrated that increasing the duration of the hold time from 180 s to 1800 s did not significantly reduce the cycle life, indicating that the number of cycles to failure in creep-fatigue reaches saturation and is independent of increasing hold time.

However, creep-fatigue evaluation using the SMT methodology takes into account stress and strain redistribution in a component due to elastic follow-up. In our previous experimental study (Wang, et.al., 2013b), it is demonstrated the elastic follow-up results in: 1) retardation of stress relaxation during hold and therefore accelerates creep damage, and 2) a non-linear increase in localized strain accumulation. The effect of hold time on SMT is therefore evaluated in this report in support of the goal of developing of SMT based creep-fatigue design curves with extrapolation to hold times representative of operation conditions (~1,000 hr of hold time).

Two SMT creep-fatigue tests were performed with Type 1 geometry with tension hold times of 1800 s (30 min) for test #37 and 36,000 s (10 hr) for test #38 at 950 ^{0}C. Both tests had an elastically calculated strain range of 0.3%. The 10 hr hold time test is the longest hold time test for Alloy 617 at 950 ^{0}C. Shown in Fig. 8 and Fig. 9 are plots of the measured strain range and maximum (tension) and minimum (compressive) stress as a function of cycle number, representative hysteresis loops, stress history, ratcheting strain and picture of the failed specimen test #37 and #38. The SMT #37 failed at about 230 cycles or 115.8 hr. Test #37 had SMT creep-fatigue life of 150 cycles or 1500.5 hr. The average strains measured at the necked test section were found to be ratcheting to the compression direction for both tests, and the specimens both failed at the transition radius with noticeable barreling.
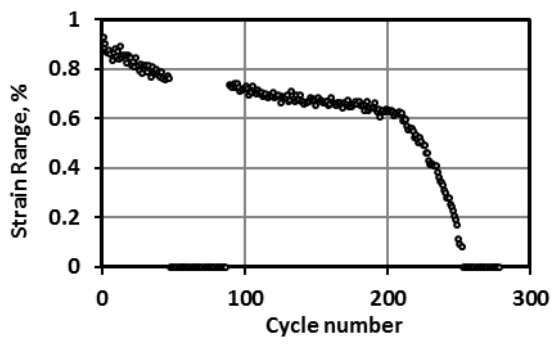
(a) Strain range
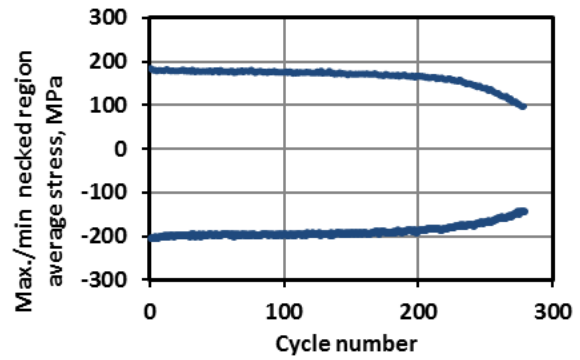
(b) Max/Min stresses
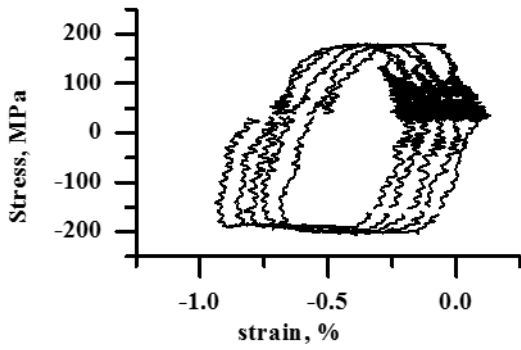
(c) Hysteresis Loop
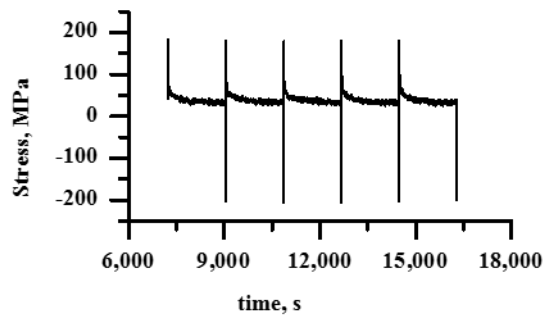
(d) Stress relaxation
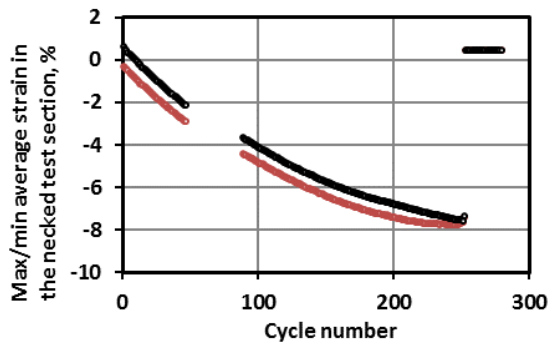
(e) Ratcheting strain
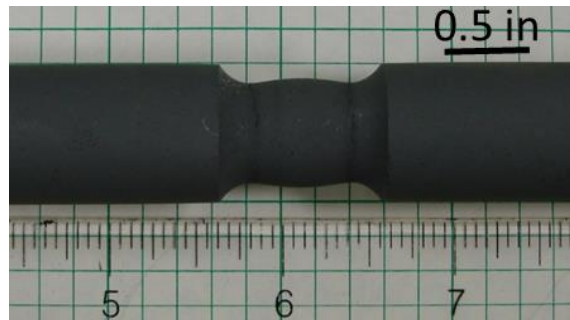
(f) Failed specimen

Fig. 8. Test results for SMT #37.

10

(a) Strain range

(b) Max/Min stresses

(c) Hysteresis Loop

(d) Stress relaxation

(e) Ratcheting strain

(f) Failed specimen
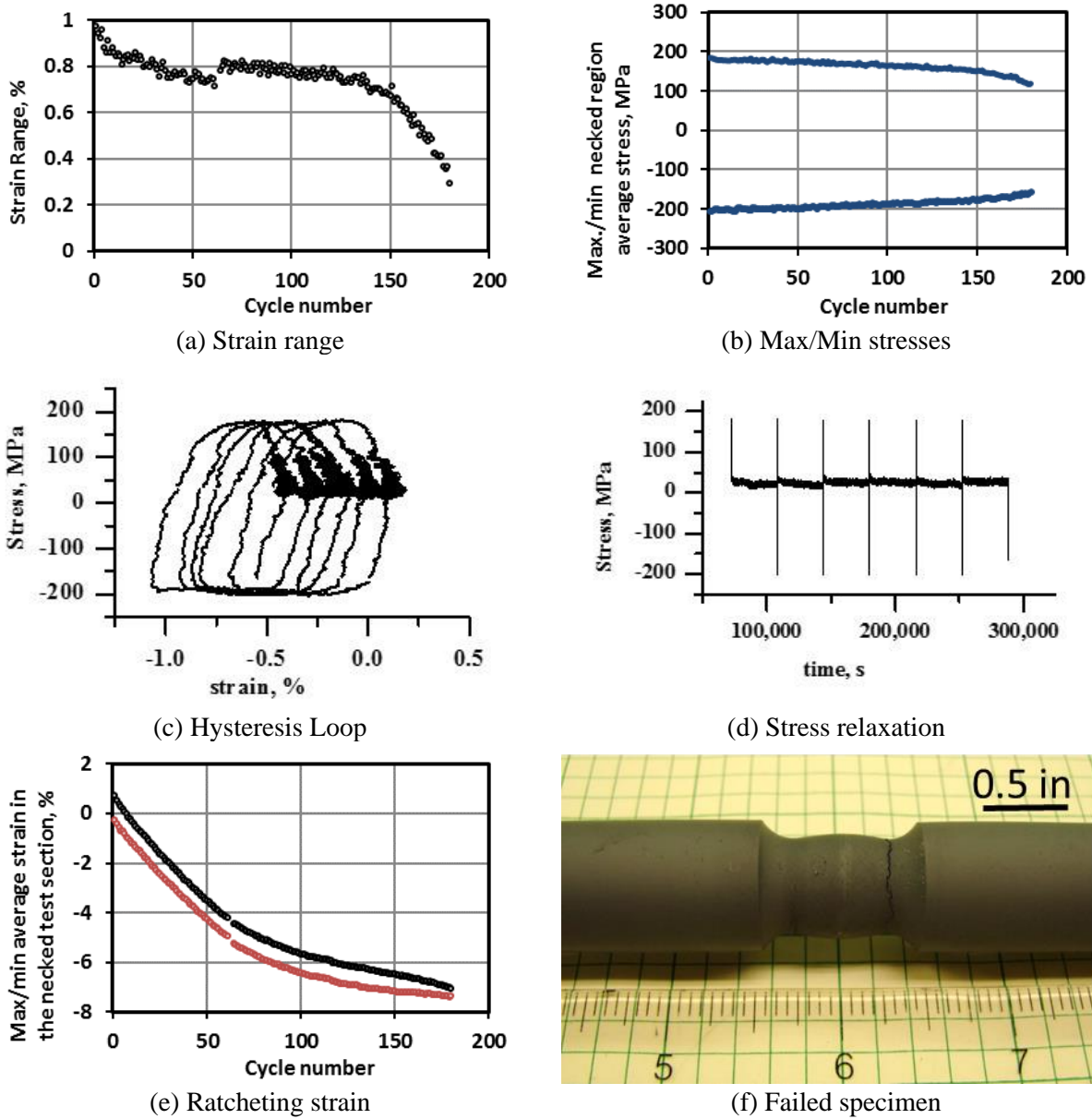
Fig. 9. Test results for SMT #38.

The test results are summarized and compared with previous test results with hold time of 600 s (10 min) in Table 4. When the hold time increased from 10 min to 30 min, the cycles to failure are reduced by 50%. The 10 hr hold time test showed the lowest cycles to failure, 150, corresponding to a reduction factor of 67% when compared to the test with 10 min hold time. The measured strain ranges were larger when the hold time was longer. Although the 10 hr hold time test has the shortest cycles, it does have the longest total test duration, followed by test # 37 with 30 min hold. The 10 min hold time test only had less than 80 hr of cycle life.

11

Table 4. Effect of tension hold times on Type 1 SMT for Alloy 617 at 950 ^{0}C.

Test #	Elastically calculated strain range	Loading time, s	Hold time, s	Initial strain range,	Failure location	Life time, hr	Cycle to failure
#1			600	0.65%		78.2	460
#2	0.3%	3	600	0.63%	Transition radius	76.5	450
#37			1,800	0.95%		115.8	230
#38			36,000	0.91%		1500.5	150

The maximum (tension) and minimum (compressive) stresses, the measured strain and strain range as a function of cycle number and equivalent cycle time are compared for test #2, #37 and #38 in Fig. 10 to demonstrate the effect of hold time on SMT creep-fatigue. The data were shown as a function of cycle number and as a function of the cycle time, to provide different perspectives while comparing these three hold time tests. The stress range of 30 min hold time test and 10 hr hold time test were the same and were larger than what was shown with 10 min hold test. When the peak stresses of the three hold time tests were compared as a function of cycle time, the degradation rate of the peak stresses was the same before showing a sharp drop prior to failure. All three hold time tests showed ratcheting toward the compression direction. The ratcheting rates as a function of cycle time were the same for the two tests with 10 min hold and 30 min hold. The strain ranges were found to continuously decrease at the same rate before the sharp drop prior to failure.
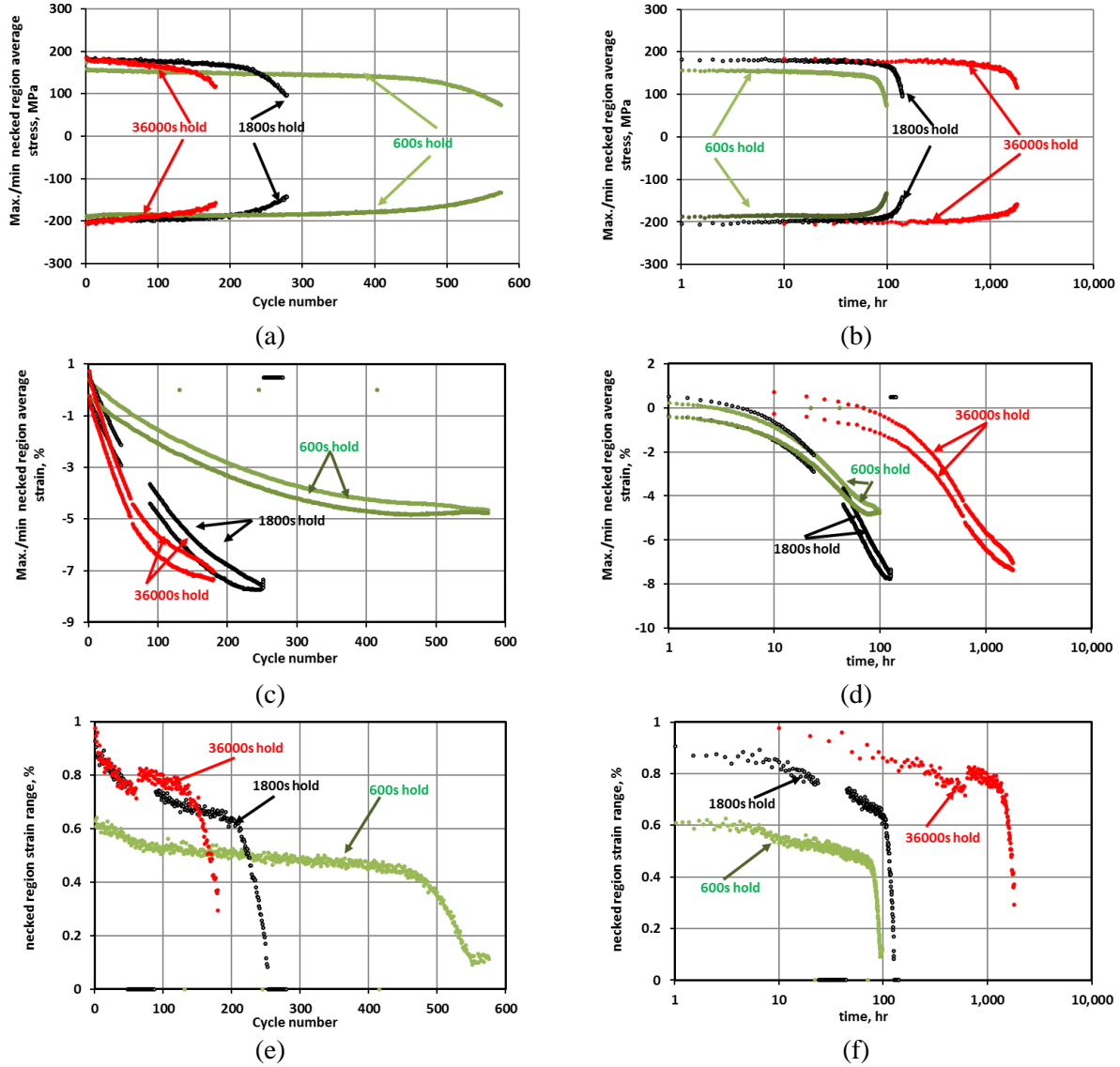
Fig. 10. Effect of hold time on Type 1 SMT creep-fatigue life of Alloy 617.

3.1.2 SMT pressurization testing on Alloy 617

SMT pressurization tests are being used to assess whether the effects of stress levels associated with sustained primary loads will be small when compared to the cyclic secondary and peak levels for the development of SMT creep-fatigue based design curve. In FY17, two additional SMT pressurization tests were performed on Alloy 617. The testing parameters and the results of these two tests are highlighted in Table 5 and Table 6 along with previous pressurized SMT results for comparison.

Table 5. Tubular SMT pressurization for Alloy 617.

Specimen ID	Amplitude, δ value	loading condition	Initial strain range	Test temperature °C	Internal pressure	Life time, hr	Cycles to failure
INC617-P01	4.5 mil	Tension hold 600 s	0.8%	950	2 psi	37.4	220
INC617-P02	4.5mil	Tension hold 600 s	0.8%	959	200 psi	37.4	220
INC617-P04	4.5mil	Tension hold 600 s	0.8%	957	500 psi	34	200
INC617-P03	4.5mil	Tension hold 600 s	0.75%	958	750 psi	25.5	150
INC617-P06	4.5mil	Tension hold 600 s	0.8%	950	750 psi	23.8	140
INC617-P09	3 mil	Tension hold 600 s	---	953	750 psi	54.4	320
INC617-P05	4.5mil	Combined tension and compression	1%	955	2psi	107.7	320
INC617-P08	4.5mil	Combined tension and compression	1.05%	950	500psi	94.3	280
INC617-P07	4.5mil	Combined tension and compression	1.05%	950	750psi	60.6	180

Table 6. Comparison of the pressurization SMT on Alloy 617.

| Specimen ID	Internal pressure	Original ID/OD	Original wall thickness	Max OD after testing	Wall thickness after failure	Failure location	Elastic follow-up factor
Tension hold SMT							
INC617-P01	2 psi	0.5in/0.62in	60mil	~0.68in	~68mil	Center	~3.8
INC617-P02	200 psi	0.5in/0.62in	60mil	~0.72in	~62mil	Center	~3.8
INC617-P04	500 psi	0.5in/0.62in	60mil	~0.75in	~54mil	Center	~4.0
INC617-P03	750 psi	0.5in/0.62in	60mil	~0.81in	~41mil	Transition radius	~4.1
INC617-P06	750 psi	0.5in/0.62in	60mil	~0.80in	~42mil	Transition radius	~4.1
INC617-P09	750 psi	0.5in/0.62in	60mil	~0.78in	~42mil	Transition radius	---
Combined Tension and Compression hold SMT							
INC617-P05	2psi	0.5in/0.62in	60mil	~0.64in	59 to 62mil	Center	---
INC617-P08	550 psi	0.5in/0.62in	60mil	~0.92in	50 to 35mil	All over	---
INC617-P07	750 psi	0.5in/0.62in	60mil	~0.95in	43 to 34mil	All over	---

INC617-P08 was tested at internal pressure of 500 psi and with combined tension and compression holds of 10min each. The 4.5mil loading amplitude over the 5 in control length for this test corresponds to an elastically calculated strain range of 0.3% inside the necked test section. At 950 ^{0}C, the initial strain range measured was shown to be approximately the same as those tested at a higher internal pressure of 750 psi and a lower internal pressure of 2psi. At 4.5 mil loading amplitude, the strain ranges with combined tension and compression loading are about 0.2% larger than those tested with tension hold for 10min. The specimen failed at ~280 cycles or 94.3 hr, shorter than INC617-P05 which was tested with 2 psi internal pressure but longer than INC617-P07 which was tested with 750 psi internal pressure. Shown in Fig. 11 are plots of the measured strain range and maximum (tension) and minimum (compressive) stress as a function of cycle number, representative hysteresis loops, stress history, ratcheting strain and picture of the failed specimen. The average strain measured at the necked test section did not change for the first 70 cycles before ratcheting to the tensile direction, and exceeded 1% ratcheting strain limits after 120 cycles of testing.
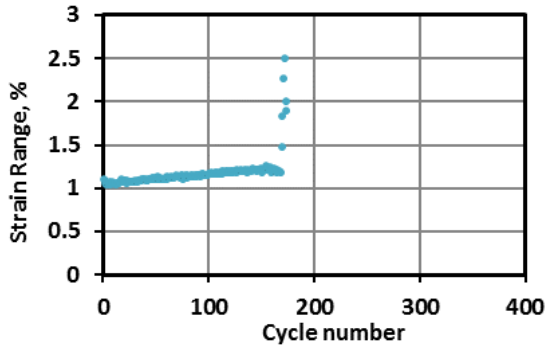
(a) Strain range
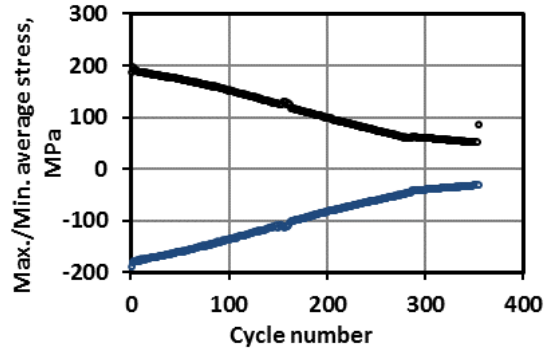
(b) Max/Min stresses
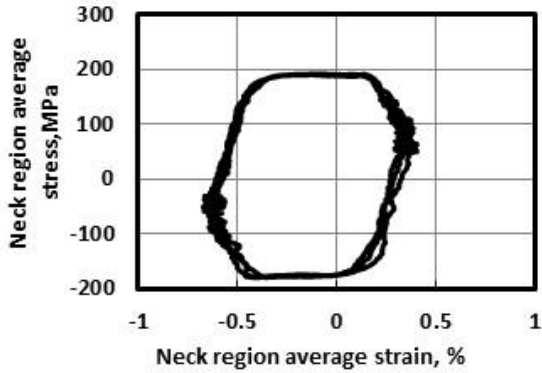
(c) Hysteresis Loop
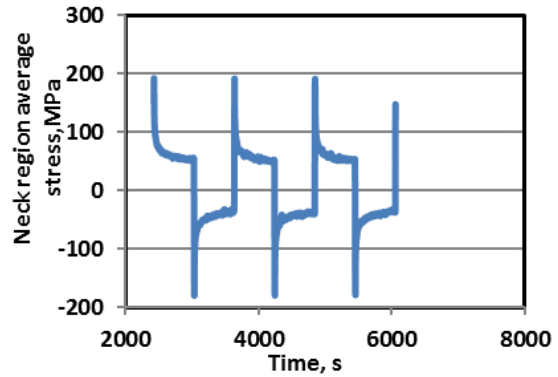
(d) Stress relaxation
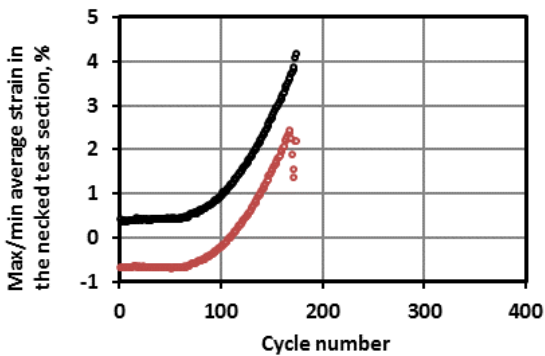
(e) Ratcheting strain
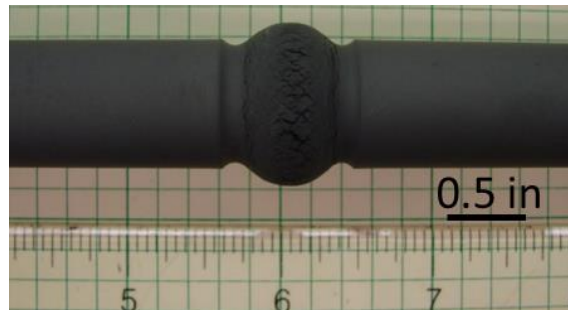
(f) Failed specimen

Fig. 11. Pressurized SMT test results for Inc617-P08.

The maximum (tension) and minimum (compressive) stresses as a function of cycle number with combined tension and compression hold for the three pressurized SMT tests are compared in Fig. 12. The SMT creep fatigue life was reduced by ~43% when the internal pressure was increased from 2 psi to 750 psi.
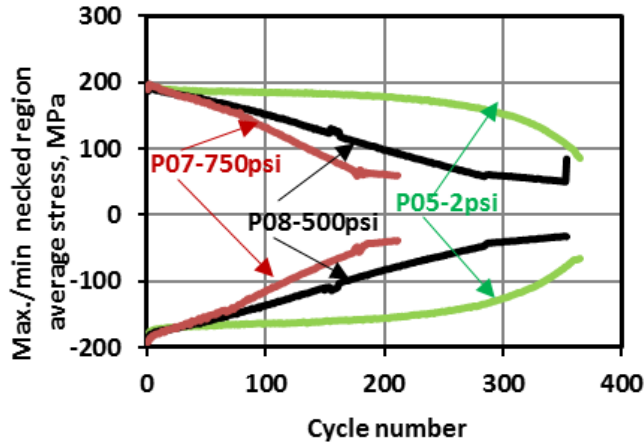
Fig. 12. Effect of internal pressure on SMT with combined tension and compression hold at 950 ^{0}C.

INC617-P09 was tested with 750 psi internal pressure at 950 ^{0}C with a lower displacement amplitude of 3 mils over the 5 in control length with tension hold of 10 min. The 3 mils amplitude corresponds to an elastically calculated strain range of 0.2% in the necked test section. It showed SMT creep-fatigue life of 320 cycles or 54.4 hr, about a factor of two when compared to those tested at 4.5 mils amplitude, a reduction ratio similar to what was shown on Type 1 SMT when tested at these two loading levels. The measurement extensometer was not responding properly for this test and only the plot of maximum (tension) and minimum (compressive) stress as a function of cycle number is presented in Fig. 13. The stress response is used as the reference for selection of the failure cycle for this test. A picture of the failed specimen is also shown in Fig. 13. It is noted that the failure location is at the transition radius region where the geometry discontinuity acted as the stress riser. The failure plane is perpendicular to the axial loading direction. For all the tension hold only tests performed on Alloy 617 at 950 ^{0}C (see Table 5 and Table 6), the failure planes are all perpendicular to the axial loading direction and not a longitudinal crack as seen in straight pressurized tests, even at the high internal pressure level of 750 psi. This indicates that the cyclic failure mode dominates even at 750psi.
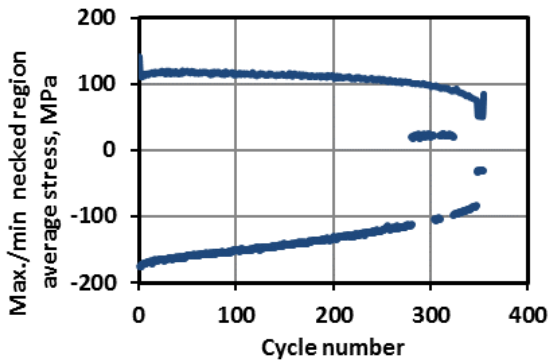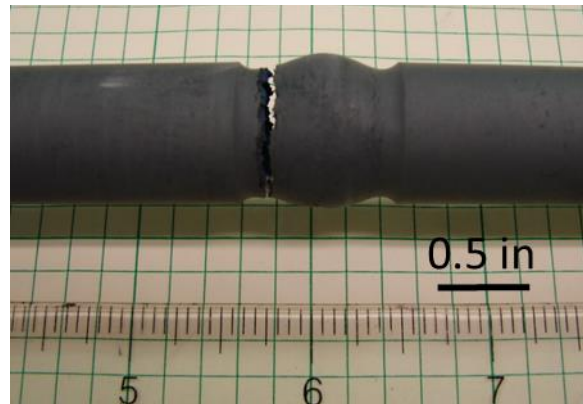
(a)Max/Min stresses   (b) Failed specimen

Fig. 13. Pressurized SMT test results for Inc617-P09.

16

Based on the results tabulated in Table 5, it is clear that higher pressures can reduce the number of cycles to failure. However, those pressures may be unrealistically high for normal operating pressure limitations. This potential limitation was assessed by determining the allowable life for pressurized cylinders using the Alloy 617 allowable stress values from a proposed Code Case for Alloy 617 (RC No. 16-994 and 16-1001). A plot of the allowable pressure vs design life for Alloy 617 at 950 ^{0}C for this testing geometry is shown in Fig. 14, with these three tested pressures highlighted in red. At 200 psi the allowable life is approximately 22,000 hr, at 500 psi about 320 hr and only about 60 hr at 750 psi. This supports the argument that, for normal design lives of about 30 years with allowable pressure of ~150 psi, the primary stress evaluation will screen out high pressures that would compromise cyclic life. Clearly additional testing at other strain ranges, temperatures and hold times will be required, but the initial results are encouraging. (Wang, et. al., 2017a).
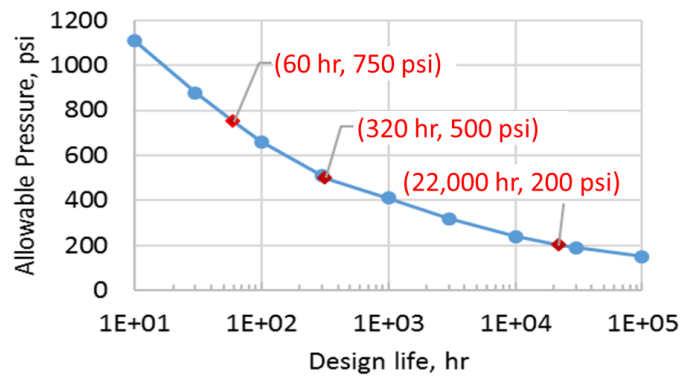
Fig. 14. Allowable pressure vs design life for Alloy 617 at 950 ºC

3.2 TWO-BAR THERMAL RACHETING EXPERIMENTAL AND ANALYTICAL RESULTS ON SS316H

Two-bar thermal ratcheting tests were performed on SS316H to assess the material response to cyclic thermal loading under two-bar testing conditions at this intermediate temperature range of 405 – 705ºC. An example of the thermal profile for one cycle is shown in Fig. 15 for testing condition with a 10 min time delay.
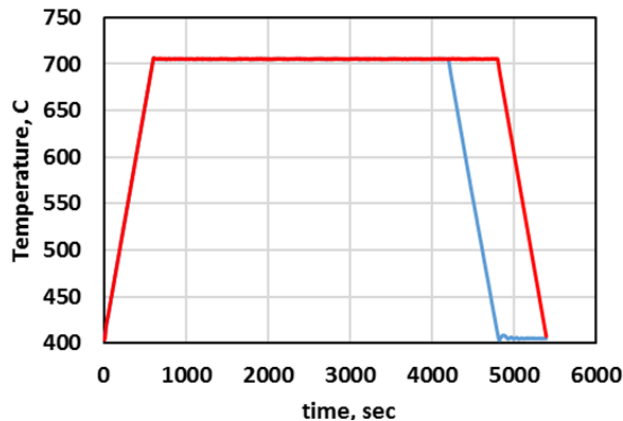
Fig. 15. An example of the thermal profile with 10 mins time delay.

17

The experiments were performed on the same set of specimens with sequential test number of T25s-1 to T25s-13. The last test in this group of testing, T25s-13, was with total load of -550lbs at 5-min delay, but it caused buckling of the specimens after 20 cycles due to excessive compressive ratcheting strain accumulation, i.e., based on the available cycles this loading condition would have caused the strain accumulation much greater than -1% for a 200 hr projected testing duration. Test T27-1 was performed on a new set of specimens with total load of 450lbs at 5-min delay. The test parameters and the test results for all the testing conditions except for T25s-13 are summarized in Table 7.

Table 7. Summary of the two-bar thermal ratcheting experiments on SS316H for temperature range of 405 ^{0}C to 705°C.

Test No.	T25s-1	T25s-2	T25s-3	T25s-4	T25s-5	T25s-6	T25s-7
Applied mean stress, MPa	3.6±0.9	10.4 ±1.0	21.1±1.0	31.5±1.0	-7.3±1.0	-7.3±1.0	-17.8±1.0
Time delay, min	10	10	10	10	5	10	3
Nominal total load, lbs	50	150	300	450	-100	-100	-250
Total No. of cycles tested	33	33	32	32	49	35	48
Ratcheting rate (per cycle), %	-0.004	-0.0006	*0.0035*	0.039	-0.0013	-0.017	-0.0005
Initial stress on Bar 1, MPa	4.6	-161.5	-136	-106.8	-138.7	-145.4	-179.4
Initial stress on Bar 2, MPa	2.4	183.7	179.1	169.2	123.9	130.8	141.3
Initial residual total strain, %	0	-0.35	-0.34	-0.12	1.23	1.11	0.31
Reference cycle No.	6	6	6	6	6	6	6
Min. total strain of the reference cycle, %	-0.24	-0.32	-0.24	0.22	1.18	0.84	0.33
Stress range per cycle for Bar 1, MPa	348.8±2.5	340.6±2.0	332.8±1.8	325.8±1.2	269.4±1.6	328.3±1.6	210.2±1.4
Stress range per cycle for Bar 2, MPa	345.1±3.0	335.9±1.8	328.2±1.5	321.3±0.6	265.1±1.2	323.5±1.2	205.9±1.0

Table 7. continue

Test No.	T25s-8	T25s-9	T25s-10	T25s-11	T25s-12	T27-1
Applied mean stress, MPa	38.9±1.0	-38.8±1.0	-18.2±1.0	-7.9±0.8	31.6±0.8	31.7±1.1
Time delay, min	3	3	5	8	7	5
Nominal total load, lbs	550	-550	-250	-100	450	450
Total No. of cycles tested	36	33	38	46	33	25
Ratcheting rate (per cycle), %	0.0014	-0.0019	*-0.003*	-0.008	0.03	0.002
Initial stress on Bar 1, MPa	-61.8	-75.4	-113.7	-135.2	-90.9	-4.3
Initial stress on Bar 2, MPa	141.3	-1.9	78.0	119.5	155.3	6.0
Initial residual total strain, %	0.33	0.29	0.27	0.13	-0.25	0
Reference cycle No.	6	6	6	6	6	6
Min. total strain of the reference cycle, %	0.4	0.32	0.23	0.047	0.11	0.076
Stress range per cycle for Bar 1, MPa	210.3±0.9	206.9±1.1	266.8±1.1	299.8±1.0	292.5±1.1	287.6±1.7
Stress range per cycle for Bar 2, MPa	206.5±1.1	202.6±1.0	262.8±0.9	297±0.8	289.9±0.8	283.1±1.9

Shown below in Fig. 16 is the envelope of loading conditions that pass the EPP strain limits code case (ASME B&PV Code Case N-861). The ordinate is the time delay in minutes as defined in Fig. 7 and the abscissa is the total applied load for the two bars with 0.25 in diameter. The analytic boundaries shown in red and blue are incremental solutions to this two-bar problem using the strain limits code case procedure. The red boundary is determined from incremental changes in the applied total load that reduce ratcheting and the blue boundary is determined from incremental changes in the applied load from inside the non-ratcheting regime that show no ratchet. The difference is due to the size of the incremental change in applied load. Also shown in Fig. 16 are the locations of the experiment test point coordinates. The circled red cross points are those that did not pass the 1% strain limits criteria and the circled green smile points are those that did.

Shown in Table 8 are the measured strain accumulations for the various test points identified in Fig. 16. There are no measured strains greater than 1% that fall within the analytically-determined strain limits boundary determined from the EPP analysis (Wang, et. al., 2017b). There are experimental points that fall outside the EPP boundary, thus indicating their conservatism. But, generally, it is shown that for points

farther outside the boundary, the strain limits are not satisfied, thus indicating that the EPP boundary is not over-conservative.

As stated above, incorporation of the SMT data-based approach for creep-fatigue damage evaluation into the EPP methodology will avoid the use of the "D" diagram and minimize over-conservatism while properly accounting for localized defects and stress risers. The plan is to use the strain range results from the EPP strain limits procedure as input to the strain range based SMT design curve. The two-bar test results can also be used to address the validity of this approach. The strain ranges of interest are those that first satisfy the EPP strain limits code case. From Fig. 16 and Table 8 the applicable strain ranges are those at a 3min delay time at -250 and 550 lb. load and a 10 min delay and 50, 150 and 300 lb load.
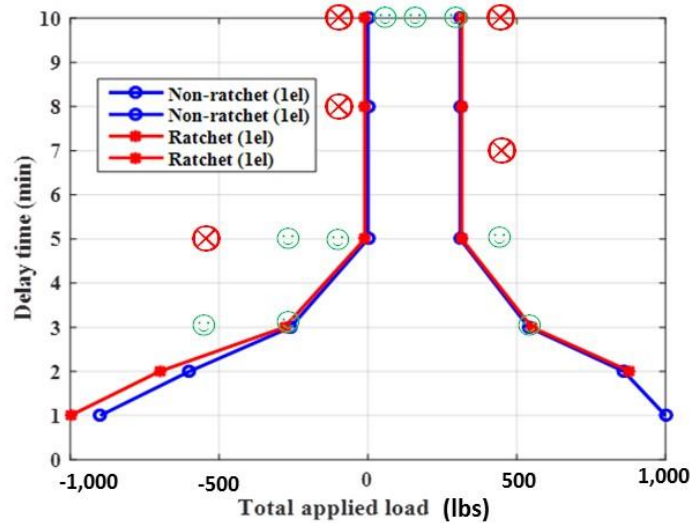

Fig. 16. EPP Strain limits envelope and test data for 405 ºC to 705 ºC temperature range (the green symbol ☺ passed 1% strain limits, while the red symbol ⊗ did not pass 1% strain limits).

Table 9 is a comparison of the experimentally measured strain range for these loading conditions to the corresponding analytically determined strain ranges from the EPP strain limits evaluation. Fig. 17 to Fig. 21 show side-by-side comparisons of the experimental and analytical hysteresis loops for Bar 1 and Bar 2. The numerical hysteresis loops are from EPP simulations of the system using 1D bar elements to represent deformation in each bar. The elastic and thermal expansion properties of the bars match those in ASME Sec. II, Part D. The temperature-dependent perfectly plastic yield stress is computed using the procedure for finding the pseudo-yield stress detailed in the EPP strain limits code case (ASME B&PV Code Case N-861). For the cases presented in the figures the system achieves plastic shakedown so a single, stable loop summarizes the steady-state system response.

As seen from Table 4, for the three cases at 10min delay, the analytic strain range is greater than the experimental range for Bar 2, the thermal lagging bar with the largest strain range. The margin is conservative but not excessive. Conversely, the experimental strain range in Bar 1, the thermal leading bar with the lower strain range, is larger than the analytic strain range, which is unconservative.

Table 8. Experimental results for 405ºC to 705ºC temperature range.

Nominal total load (lbs)	Time delay (min)	Ratcheting strain in 200 hr, %	Pass/fail 1% strain limits
-550	3	0.20%	Pass
-550	5	-8.79%	Fail
-250	3	-0.07%	Pass
-250	5	-0.47%	Pass
-100	5	-0.19%	Pass
-100	10	-2.31%	Fail
-100	8	-1.15%	Fail
50	10	-0.56%	Pass
150	10	-0.08%	Pass
300	10	0.47%	Pass
450	10	5.19%	Fail
450	7	4.18%	Fail
450	5	0.29%	Pass
550	3	0.20%	pass

For the two cases with lower strain ranges as a result of the lower delay time, the analytic strain range is slightly non-conservative in Bar 2 and more non-conservative in Bar 1. Interestingly, the experimental data show that Bar 2 had larger mechanical strain ranges while loaded at higher thermal stress with 10 min time delay, it showed smaller strain ranges than Bar 1, while at the lower loaded 3 min delay, Bar 1 experiences the greater strain range than Bar 2.

Table 9. Experimental and analytical strain ranges.

Nominal Total Load, (lbs)	Delay time, (min)	Mechanical strain range Bar 1 (%)		Mechanical strain range -Bar 2 (%)	
		Exp.	Anal.	Exp.	Anal.
-250	3	0.17	0.096	0.11	0.099
550	3	0.17	0.0982	0.11	0.099
50	10	0.32	0.183	0.41	0.49
150	10	0.30	0.183	0.41	0.49
300	10	0.30	0.184	0.42	0.493

The side-by-side plots of the hysteresis loops in Fig. 17 through Fig. 21 show good qualitative agreement between experiment and analysis. The plots on the experimental data consist of five consecutive cycles (from cycle number 10 to cycle number 14) for each condition and the plots from EPP analysis consist of first 9 to 10 cycles. Among these test conditions, for the more highly loaded cases at 10min delay, the plasticity in the Bar 2 hysteresis loops qualitatively show good agreement with the experimental loops. The experiment loops in Bar 1 show slight inelasticity, closely approximating the elastic behavior from the analysis. For the more lightly loaded 3 min delay cases, both the experimental and analytic loops in both bars show elastic behavior; although, there was an as yet unexplained kink in the Bar 2 response. (Wang, et. al., 2017b).)

Although the hysteresis loops are compatible and the agreement between experiment and analysis is not unreasonably conservative for the higher load cases and larger strain ranges, the non-conservatism at lower loads and strain ranges warrants additional investigation.

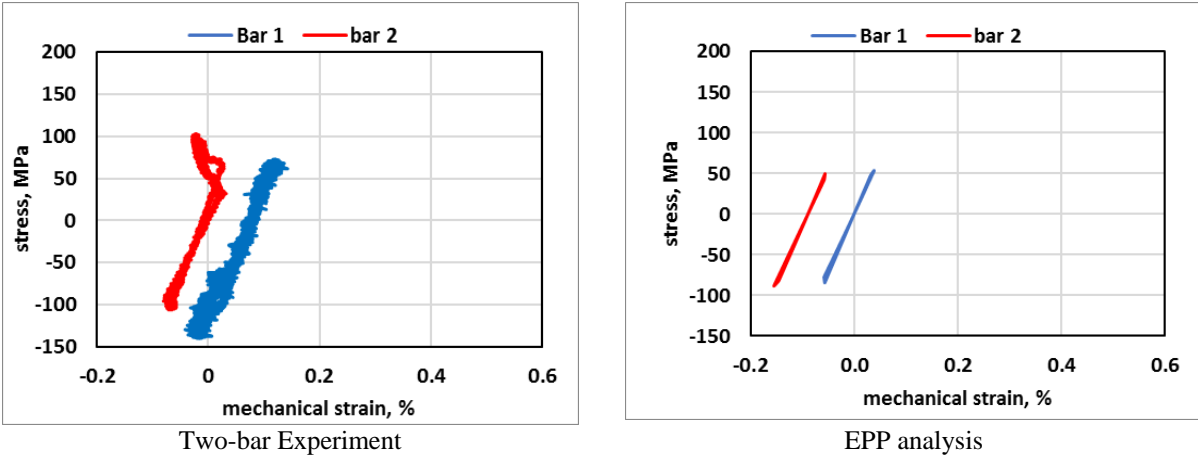|	
Two-bar Experiment	EPP analysis

Fig. 17. Hysteresis loops of the two bars with -250 lb and 3 min delay loading condition.

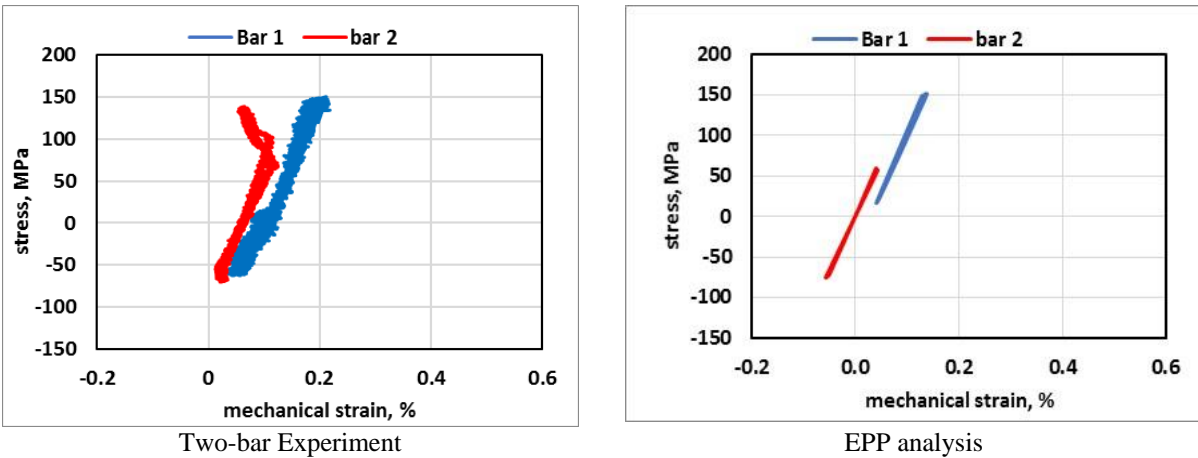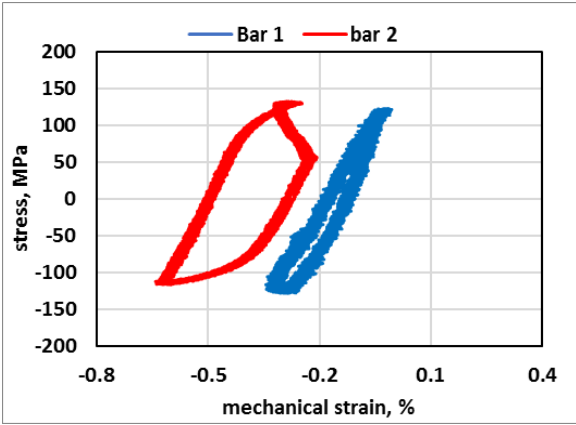|	
Two-bar Experiment	EPP analysis

Fig. 18. Hysteresis loops of the two bars with 550 lb and 3 min delay loading condition.

Two-bar Experiment   EPP analysis
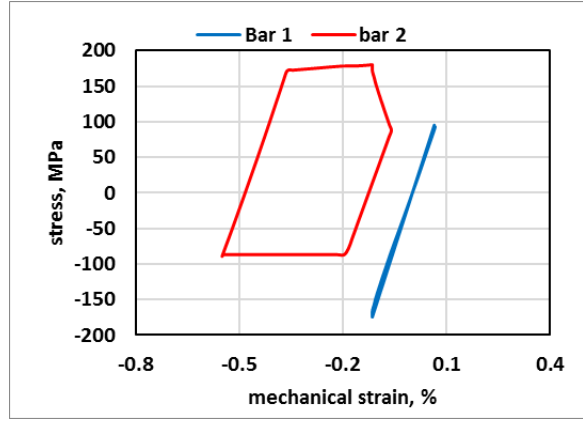
Fig. 19. Hysteresis loops of the two bars with 50 lb and 10 min delay loading condition.
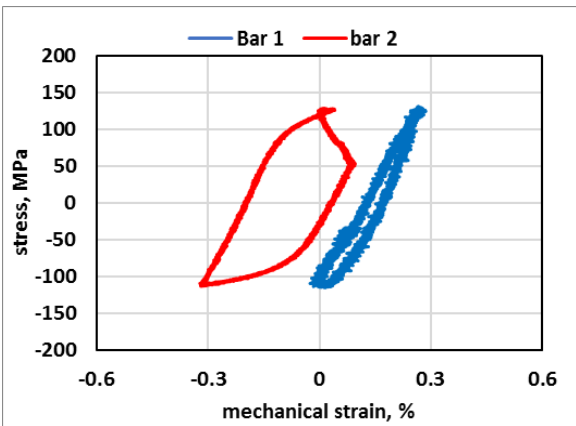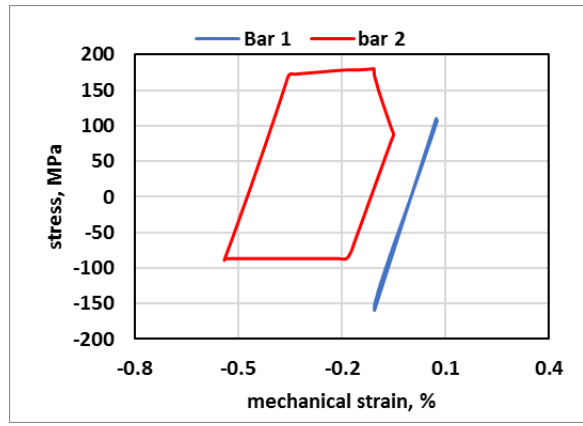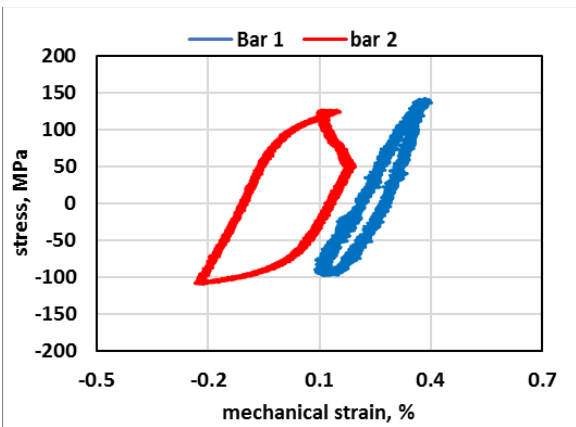

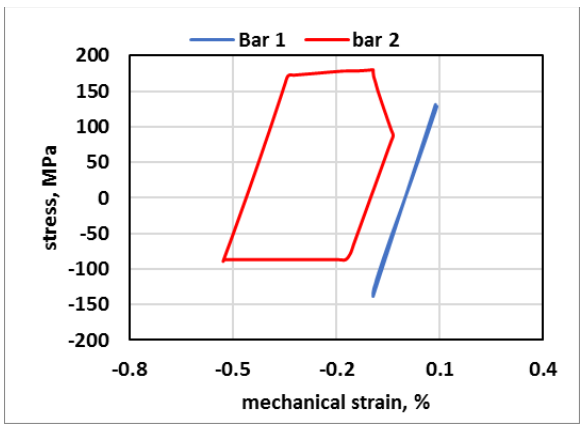Two-bar Experiment   EPP analysis

Fig. 20. Hysteresis loops of the two bars with 150 lb and 10 min delay loading condition.

Two-bar Experiment   EPP analysis

Fig. 21. Hysteresis loops of the two bars with 300 lb and 10 min delay loading condition.

23

4. SUMMARY

The development of the integrated EPP combined SMT creep-fatigue damage evaluation approach is reported. The goal of the proposed approach is to combine the advantage of the EPP strain limits methodology that avoids stress classification with the advantage of the SMT method for evaluating creep-fatigue damage without deconstructing the cyclic history into separate fatigue and creep damage evaluations. In support of the development of this methodology in FY17, experiments were performed on Alloy 617 with longer tension hold times of 30 min and 10 hr at 950 ^{0}C. The enhanced damage resulting from strain redistribution and slowed stress relaxation due to follow up effects was demonstrated in the test results. Although standard strain controlled creep-fatigue on smooth bar showed saturation at 180 s hold time, the SMT test with 30 min hold time did not show saturation. The test with hold time of 10 hr showed a reduction of creep-fatigue cycles by 67% when compared to the test with 10 min hold time.

Pressurized SMT specimens on Alloy 617 were used to assess the role of sustained primary loading on cyclic life. Although high pressures reduced cyclic life, it was shown that such high pressure levels would not be permissible under normal design limitations on pressure as a function of service life.

Two-bar thermal ratcheting tests were conducted on 316H stainless steel specimens with an applied temperature transient from 405 to 705°C at several constant applied combined total loads. These test data points were then evaluated analytically using the EPP strain limits procedures and compared to the 1% EPP strain limits boundary. There were no measured strains greater than 1% that fell within the analytically determined strain limits boundary. Although there were experimental points that fell outside the EPP boundary, generally, it was shown that the EPP boundary was not over-conservative. Regarding the strain range assessment, the experimental and analytic hysteresis loops were qualitatively compatible. The agreement between experimental and analytical strain ranges is not unreasonably conservative for the higher load cases and larger strain ranges, but non-conservatism at lower loads and strain ranges warrants additional investigation.

REFERENCES

ASME B&PV Code Case N-861 "Satisfaction of Strain Limits for Division 5 Class A Components at Elevated Temperature Service Using Elastic-Perfectly Plastic Analysis".

ASME B&PV Code Case N-862 "Calculation of Creep-Fatigue for Division 5 Class A Components at Elevated Temperature Service Using Elastic-Perfectly Plastic Analysis Section III, Division 5"

Carroll, L. J., Cabet, C., R. Madland and Wright, R. N., (2011). "Creep and Environmental Effects on the High Temperature Creep-fatigue Behavior of Alloy 617," J*ournal of ASTM International*, Vol. 8, No. 6, pp. 1-13, https://doi.org/10.1520/JAI103797.

Swindeman, R., Robinson, D., Williams, B. and Thomas, D., (1982), "Two-Bar Thermal Ratcheting Experiments on 2¼Cr-1Mo Steel," Technical Report No. ORNL/TM-8001, Oak Ridge National Laboratory, Oak Ridge, TN.

Wang, Y., Sham, T.-L, and Jetter, R. I., (2013a), "Progress report on the development of test procedure for the two-bar thermal ratcheting experiment for Alloy 617", ORNL/TM-2013/318, Oak Ridge National Laboratory, Oak Ridge, TN.

Wang, Y., Jetter, R. I., Krishnan, K., and Sham, T.-L, (2013b) "Progress Report on Creep-Fatigue Design Method Development Based on SMT Approach for Alloy 617", ORNL/TM-2013/349, Oak Ridge National Laboratory, Oak Ridge, TN.

Wang, Y., Jetter, R. I. and Sham, T.-L, (2014), "Application of Combined Sustained and Cyclic Loading Test Results to Alloy 617 Elevated Temperature Design Criteria", ORNL/TM-2014/294, Oak Ridge National Laboratory, Oak Ridge, TN.

Wang, Y., Jetter, R. I., Baird, S. T., Pu, C. and Sham, T.-L., (2015), "Report on FY15 Two-Bar Thermal Ratcheting Test Results", ORNL/TM-2015/284, Oak Ridge National Laboratory, Oak Ridge, TN.

Wang, Y., Jetter, R. I., and Sham, T.-L., (2016), "Preliminary Test Results in Support of Integrated EPP and SMT Design Methods Development", ORNL/TM-2016/76, Oak Ridge National Laboratory, Oak Ridge, TN.

Wang, Y., Jetter, and Sham, T.-L., (2017a), "Pressurized Creep-Fatigue Testing of Alloy 617 Using Simplified Model Test Method", Proceedings of the ASME 2017 Pressure Vessels and Piping Conference, PVP2017-65457

Wang, Y., Jetter, R. I., Messner, M., Mohanty , S., and Sham, T.-L., (2017b), "Combined Load and Displacement Controlled Testing to Support Development of Simplified Component Design Rules for Elevated Temperature Service", Proceedings of the ASME 2017 Pressure Vessels and Piping Conference, PVP2017-65455

ELECTRONIC DISTRIBUTION

Name	Affiliation	Email
Corwin, W.	DOE-NE	william.corwin@nuclear.energy.gov
Gougar, H.	INL	Hans.Gougar@inl.gov
Grandy, C.	ANL	cgrandy@anl.gov
Hill, R.N.	ANL	bobhill@anl.gov
Jetter, R.I.	R.I. Jetter Consulting	bjetter@sbcglobal.net
Lara-Curzio, E.	ORNL	laracurzioe@ornl.gov
Li, D.	DOE-NE	Diana.Li@nuclear.energy.gov
Lin, L.	ORNL	linl@ornl.gov
McMurtrey, M.	INL	michael.mcmurtrey@inl.gov
Messner, M.C.	ANL	messner@anl.gov
Natesan, K.	ANL	natesan@anl.gov
Qualls, L.	ORNL	quallsal@ornl.gov
Robinson, B.	DOE-NE	Brian.Robinson@Nuclear.Energy.gov
Sham, T.-L.	ANL	ssham@anl.gov
Wang, H.	ORNL	wangh@ornl.gov
Wang, Y.	ORNL	wangy3@ornl.gov
Wright, R.N.	INL	richard.wright@inl.gov
Yankeelov, J.	DOE-ID	yankeeja@id.doe.gov